Progress In Electromagnetics Research, PIER 28, 17–28, 2000

A TWO-STEP NUMERICAL SOLUTION OF MAGNETIC FIELD PRODUCED BY ELF SOURCES WITHIN A STEEL PIPE

X.-B. Xu and G. Liu

Holcombe Electrical and Computer Engineering Department
Clemson University
Clemson, SC 29634-0915

1. Introduction
2. Finite Element Method Solution
3. Formulation of Equivalence Computational Model
4. Results and Discussions
References

1. INTRODUCTION

Recently, the investigation of extremely-low-frequency (ELF) magnetic field has drawn a lot of researchers' attention. The magnetic field of overhead power transmission lines has been studied extensively and summarized in [1] and [2]. It is also of interest to study the ELF magnetic field produced by underground pipe-type cables, which are widely used in urban areas for power transmission. In this area, the earlier work was published by Wait and Hill in 1977 [3]. They developed a computational model to predict the electromagnetic field shielding effect of a metal casing enclosing two-dimensional sources. But in their computational model, a constant permeability was assumed for the metal casing. To study the effect of a steel pipe enclosing sources, the other researchers have developed an iterative procedure to handle the nonlinearity of the steel pipe and to determine the relative permeability, which varies from point to point in the pipe. Then, knowledge of the relative permeability of the steel pipe was used in a finite-element-method solution procedure to determine the power losses, the fields

and forces in a pipe-type cable [4, 5]. Most recently, numerical techniques based on Fourier series expansion [6] and unimoment method [7, 8] have been developed for investigating the magnetic field of buried pipe-type cables. The numerical technique presented in [6] is developed under the assumption that the permeability of the steel pipe varies in the radial direction only.

In this paper, we present a two-step numerical solution technique for determining the magnetic field generated by ELF sources enclosed by a steep pipe. In the first step, finite-element method [9–11] is employed to compute the potentials and fields everywhere in the region enclosed by the pipe. In particular, the electric and magnetic fields on the outer surface of the steel pipe are determined. Then, in the second step, we employ the equivalence principle [12] to formulate a model equivalent to the region exterior to the pipe. In the equivalent model, the equivalent surface currents can be obtained *directly* from knowledge of the fields on the outer surface of the pipe. Using the equivalent surface currents, the magnetic field outside the pipe is computed. This method has its advantages comparing to the numerical methods presented in [6–8]. This method is more accurate than that developed in [6], since it can determine the permeability varying from point to point in the steel pipe, while in [6], the permeability is assumed to be a constant in each layer of the steel pipe, which is just an approximation. Also, this method is simpler than the unimoment method presented in [7, 8]. In the first step, a straightforward finite-element-method solution procedure is employed to solve the differential equations subject to a properly set homogeneous Dirichlet boundary condition. Then, in the second step, no more computation is needed for determining the equivalent currents. since they are simply equal to the corresponding field components obtained in the first step. As an example of applications of the two-step numerical technique, this technique is employed to determine the magnetic field produced by an underground pipe-type cable. To validate the proposed numerical technique, the computed results are compared with existing measurement data.

2. FINITE ELEMENT METHOD SOLUTION

In Fig. 1 is depicted a cross sectional view of an underground cable, in which the three-phase conductors are placed within a fluid-filled steel pipe enclosure. The electromagnetic properties of the fluid, the phase conductors, the shields, the pipe, and the earth are characterized by

(μ_0, ε_0), (μ_c, σ_c), (μ_s, σ_s), (μ_p, σ_p), and (μ_e, σ_e), respectively, where μ is the permeability, ε is the permittivity, and σ is the conductivity of the material. A z-directed phase current I_i $(i = a, b, c)$ flows in the phase conductors. The currents result in a z-directed magnetic vector potential A_z everywhere, which must satisfy the following differential equations,

$$\frac{\partial}{\partial x}\left(\frac{1}{\mu_0}\frac{\partial A_z}{\partial x}\right) + \frac{\partial}{\partial y}\left(\frac{1}{\mu_0}\frac{\partial A_z}{\partial y}\right) = 0, \tag{1}$$

in the fluid,

$$\frac{\partial}{\partial x}\left(\frac{1}{\mu_0}\frac{\partial A_z}{\partial x}\right) + \frac{\partial}{\partial y}\left(\frac{1}{\mu_0}\frac{\partial A_z}{\partial y}\right) - j\omega\sigma_c A_z + J_{iz}^s = 0, \tag{2a}$$

$$- j\omega\sigma_c A_z + J_{iz}^s = J_{iz}, \tag{2b}$$

and

$$\iint_{S_c} J_{iz}\, ds = I_i, \qquad i = a, b, c, \tag{2c}$$

in the phase conductors, where S_c is their cross sectional area,

$$\frac{\partial}{\partial x}\left(\frac{1}{\mu_p}\frac{\partial A_z}{\partial x}\right) + \frac{\partial}{\partial y}\left(\frac{1}{\mu_p}\frac{\partial A_z}{\partial y}\right) - j\omega\sigma_p A_z = -J_{pz}^s, \tag{3}$$

in the steel pipe,

$$\frac{\partial}{\partial x}\left(\frac{1}{\mu_0}\frac{\partial A_z}{\partial x}\right) + \frac{\partial}{\partial y}\left(\frac{1}{\mu_0}\frac{\partial A_z}{\partial y}\right) - j\omega\sigma_s A_z = -J_{sz}^s, \tag{4}$$

in the phase-conductor shields, and

$$\frac{\partial}{\partial x}\left(\frac{1}{\mu_e}\frac{\partial A_z}{\partial x}\right) + \frac{\partial}{\partial y}\left(\frac{1}{\mu_e}\frac{\partial A_z}{\partial y}\right) - j\omega\sigma_e A_z = 0, \tag{5}$$

in the earth. In equations (1)–(5), J_{iz}^s J_{pz}^s and J_{sz}^s are the source current densities in the ith conductor $(i = a, b, c)$, in the pipe, and in the shields, respectively.

To solve the differential equations (1)–(5), a finite-element mesh structure is formulated for the pipe-type cable and its vicinity. It is truncated at $\rho = R_1 > C_1$, where C_1 is the radius of the outer surface of the steel pipe. R_1 is the radius of a circular surface, determined

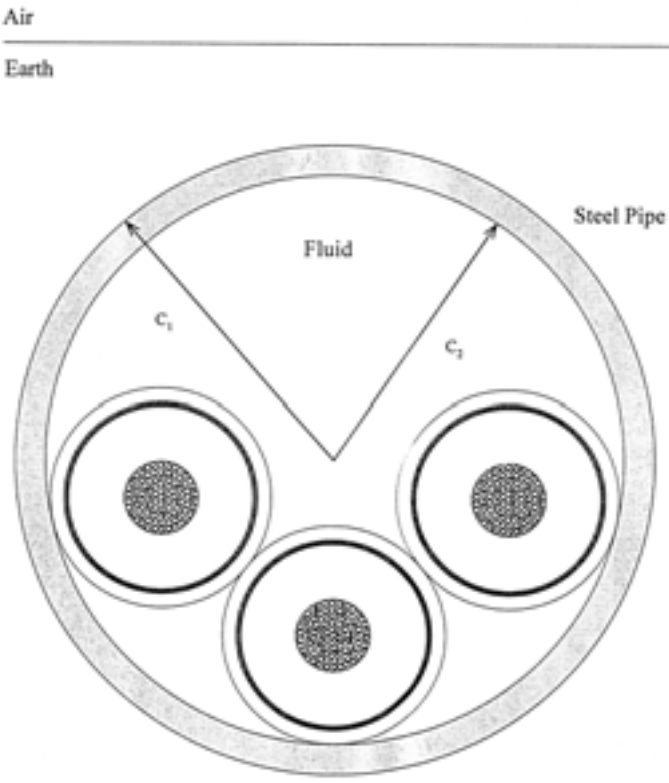

Figure 1. Cross-section of an underground three-phase pipe-type cable.

by numerical tests [11, 16], on which the magnetic vector potential is approximately constant. A homogeneous Dirichlet boundary condition [11, 13–15],

$$A_z = 0, \tag{6}$$

is set at $\rho = R_1$. Then, the finite element method is employed to solve the differential equations (1)–(5), subject to the homogeneous Dirichlet boundary condition given in (6). In the solution procedure, special attention is paid to the nonlinear B-H characteristic of the steel pipe, and an iterative procedure [4, 5, 11] is employed to determine the permeability μ_p varying in the steel pipe. The details of the finite-element-method solution of A_z are presented in [11], hence not repeated here. Based on knowledge of the magnetic vector potential A_z the electric field intensity E_z and the magnetic field intensity H_ϕ

on the outer surface of the steel pipe $(\rho = C_1)$ can be computed. The magnitude and phase of E_z and H_ϕ at $\rho = C_1$, computed for the phase current $I_i = 600A$, are shown in Figs. 2 and 3. One observes that the magnitudes of E_z and H_ϕ are symmetric about the y-axis $(\phi = 90^\circ$ and $\phi = 270^\circ)$, and their phases change signs across the y-axis, as expected.

3. FORMULATION OF EQUIVALENCE COMPUTATIONAL MODEL

Employing the equivalence principle [12], a computational model equivalent to the region exterior to the pipe-type cable is formulated and depicted in Fig. 4. The equivalent electric surface current $\vec{J}_s$ and the equivalent magnetic surface current $\vec{K}_s$ can be obtained by

$$\vec{J}_s = \hat{n} \times \vec{H},$$

or

$$J_{sz} = H_\phi, \qquad \text{at } \rho = C_1, \tag{7a}$$

and

$$\vec{K}_s = \vec{E} \times \hat{n}$$

or

$$K_{s\phi} = E_z, \qquad \text{at } \rho = C_1. \tag{7b}$$

Since E_z and H_ϕ at $\rho = C_1$ are the finite-element-method solutions already obtained in the previous section, *no* further computation is needed for determining the equivalent surface currents $\vec{J}_s$ and $\vec{K}_s$. Then, based on knowledge of the equivalent surface currents, the magnetic field at a point (x, y) of interest, produced by the pipe-type cable can be calculated by

$$\vec{H} = [H_x(J_{sz}) + H_x(K_{s\phi})]\,\hat{x} + [H_y(J_{sz}) + H_y(K_{s\phi})]\,\hat{y}, \tag{8}$$

where

$$H_x(J_{sz}) = -\frac{1}{2\pi}\int_{C_1} J_{sz}(\ell')\frac{y - y'}{(x - x')^2 + (y - y')^2}d\ell', \tag{9a}$$

$$H_y(J_{sz}) = -\frac{1}{2\pi}\int_{C^1} J_{sz}(\ell')\frac{x - x'}{(x - x')^2 + (y - y')^2}d\ell', \tag{9b}$$

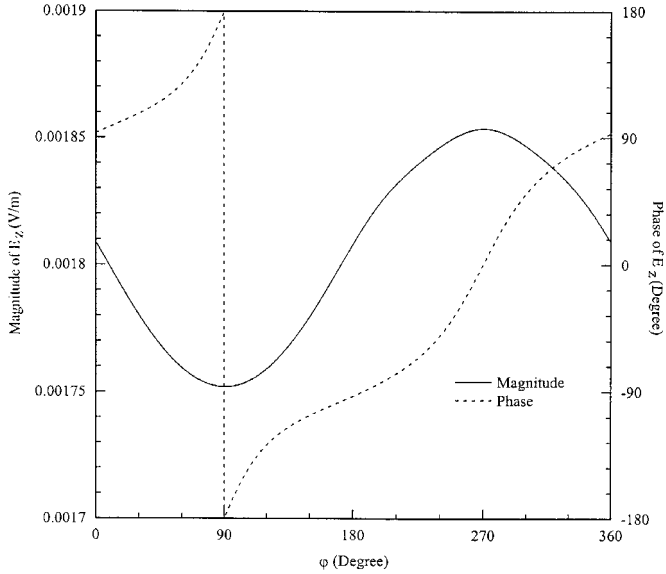

Figure 2. Finite-element-method solution of the electric field intensity E_z , in magnitude and phase, on the outer surface of the steel pipe, computed for the phase current $I_i = 600A$.

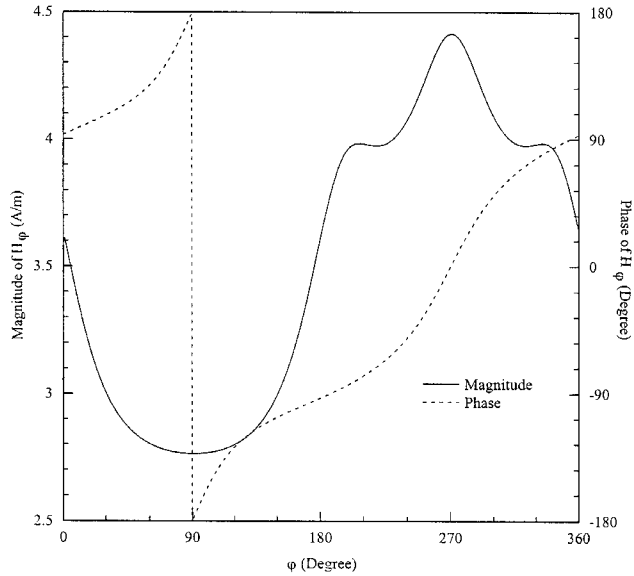

Figure 3. Finite-element-method solution of the magnetic field intensity H_ϕ , in magnitude and phase, on the outer surface of the steel pipe, computed for the phase current $I_i = 600A$.

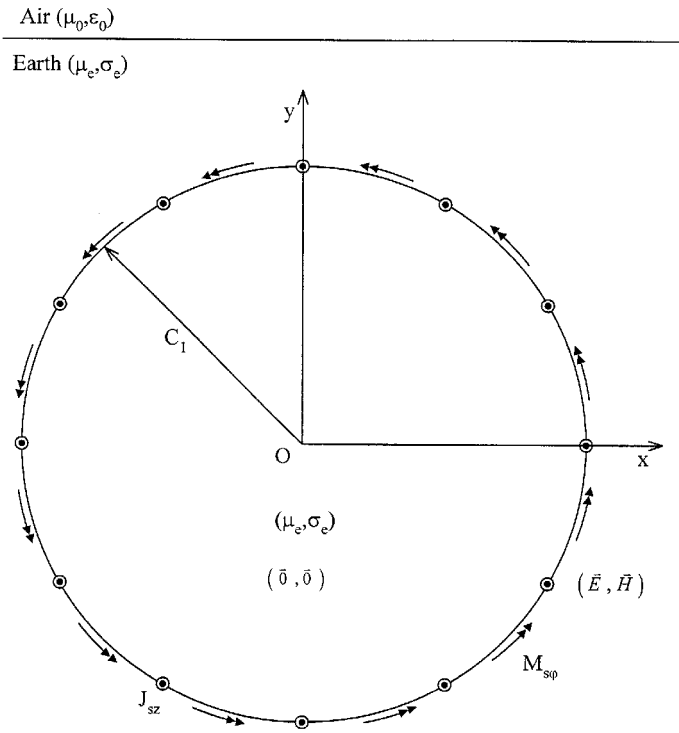

Figure 4. Computational model equivalent to the region external to the pipe-type cable.

at ELF and

$$H_x(K_{s\phi}) = -\sigma_e \int_{C_1} K_{sx}(\ell') G_e(\vec{\rho},\vec{\rho}')d\ell' - \frac{\sigma_e}{k_e^2} \cdot \int_{C_1} \left[K_{sx}(\ell') \frac{\partial^2 G_e(\vec{\rho},\vec{\rho}')}{\partial x^2} + K_{sy}(\ell') \frac{\partial^2 G_e(\vec{\rho},\vec{\rho}')}{\partial x \partial y} \right] d\ell', \quad (9c)$$

$$H_y(K_1) = -\sigma_e \int_{C_1} K_{sy}(\ell') G_e(\vec{\rho},\vec{\rho}')d\ell' - \frac{\sigma_e}{k_e^2} \cdot \int_{C_1} \left[K_{sx}(\ell') \frac{\partial^2 G_e(\vec{\rho},\vec{\rho}')}{\partial x \partial y} + K_{sy}(\ell') \frac{\partial^2 G_e(\vec{\rho},\vec{\rho}')}{\partial y^2} \right] d\ell'. \quad (9d)$$

In equations (9c) and (9d), the Green's function $G_e(\vec{\rho},\vec{\rho}')$ is defined by

$$G_e(\vec{\rho},\vec{\rho}') = -\frac{j}{4} H_0^{(2)} \left(k_e |\vec{\rho} - \vec{\rho}'| \right), \quad (10)$$

in which $H_0(\cdot)$ is the zero-order Hankel function of the second kind and k_e is the wave number of the Earth. At ELF, the Green's function reduces to

$$G_e(\vec{\rho}, \vec{\rho}') = -\frac{j}{4}\left[1 - \frac{j2}{\pi}\ln\left(\frac{\gamma|\vec{\rho} - \vec{\rho}'|}{2}\right)\right], \qquad (10')$$

in which $\gamma = 1.781$.

4. RESULTS AND DISCUSSIONS

The two-step numerical technique presented in this paper can be employed for determining the magnetic field produced by sources in arbitrary configuration enclosed by a ferromagnetic pipe. In this section, however, we only present the numerical results, as an example, of the magnetic field in the vicinity of an underground three-phase pipe-type cable. The pipe-type cable investigated has three phase conductors placed within a $10''$ steel pipe ($C_1 = 0.136\,\text{m}$, $C_2 = 0.130\,\text{m}$) in cradle configuration. The B-H curve of the steel pipe is shown in [6]. To validate the numerical technique presented, its results are compared with the existing measurement data, as well as the Fourier series method results [6].

In Figs. 5(a) and 5(b) are shown comparisons of the numerical results of the two-step numerical technique (TSNT) presented in this paper and that of the Fourier series method (FSM), as well as the measurement data of the magnetic flux density distribution along a horizontal line at different height $h = 0.5\,\text{m}$ and $h = 1.04\,\text{m}$ above the pipe-type cable. The pipe-type cable carries a balanced current of 600 A. The comparisons show that the numerical results of the two-step numerical technique agree with the measurement data. Moreover, one observes that the two-step numerical technique results agree with the measurement data better than the Fourier series method [6] results do, as one would expect. This is because that the numerical technique presented in this paper can more accurately model the nonlinear characteristic of the steel pipe, in the sense that it can determine the permeability varying from point to point in the steel pipe. But the Fourier series technique presented in [6] assumes a constant permeability in each layer of the steel pipe, which is just an approximation. Similar comparisons are depicted in Figs. 6(a) and 6(b) for the pipe-type cable carrying a balance current of 900 A. From these comparisons, the same observation can be made as that made from Figs. 5(a) and 5(b).

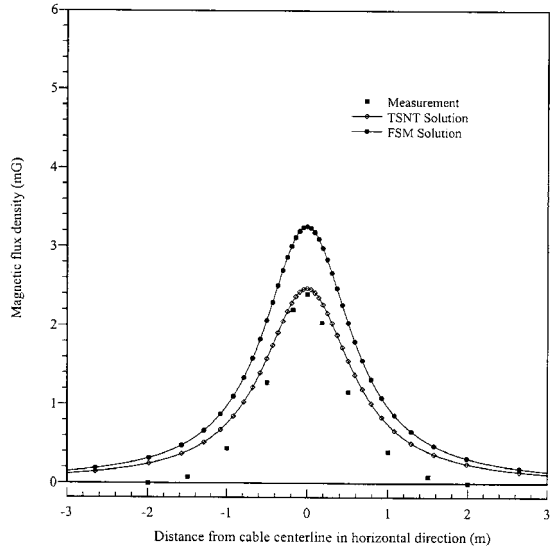

(a) $h = 0.5$ m

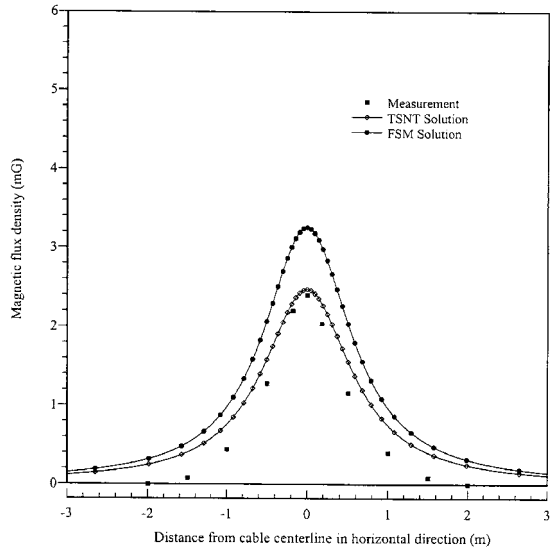

(b) $h = 1.4$ m

Figure 5. Comparison of Numerical Results of the Two-Step Numerical Technique (TSNT) and that of Fourier Series Method (FSM), as well as the Measurement Data of Magnetic Flux Density Distribution along a Horizontal Line at Different Height above the Pipe-Type Cable, for $I = 600$ A.

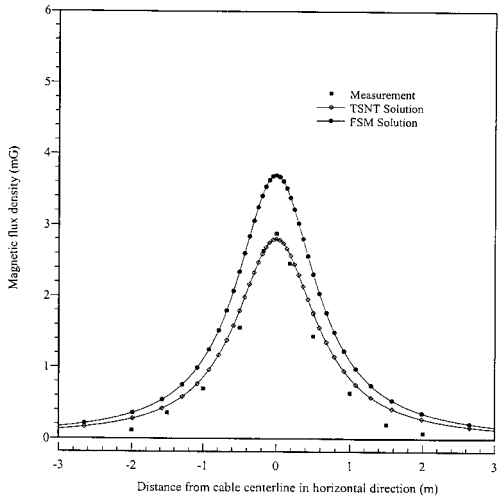

(a) $h = 0.5$ m

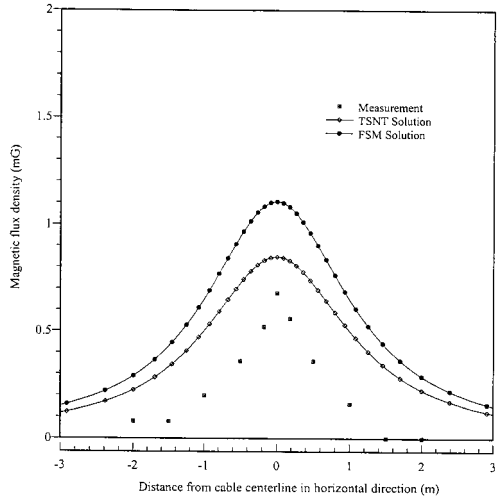

(b) $h = 1.4$ m

Figure 6. Comparison of Numerical Results of the Two-Step Numerical Technique (TSNT) and that of Fourier Series Method (FSM), as well as the Measurement Data of Magnetic Flux Density Distribution along a Horizontal Line at Different Height above the Pipe-Type Cable, for $I = 900$ A.

ACKNOWLEDGMENT

The authors appreciate the financial support to this work, provided by National Science Foundation under the award number ECS-9632118.

REFERENCES

1. Olsen, R. G., and V. L. Chartier, "The performance of reduced magnetic field power lines theory and measurements on an operating line," *92 SM458-D PWRD,* 1–11, IEEE/PES1992 Summer Meeting, Seattle, WA, July 12–16, 1992.
2. Moore, T., "Exploring the options for magnetic field management," *EPRI Journal,* Vol. 15, No. 6, 4–19, October/November 1990.
3. Wait, J. R., and D. A. Hill, "Electromagnetic shielding of sources within a metal-cased bore hole," *IEEE Transactions on Geoscience Electronics,* Vol. GE-15, No. 2, 108–112, April 1977.
4. Labridis, D., and P. Dokopoulos, "Finite element computation of field, losses and forces in a three-phase gas cable with nonsymmetrical conductor arrangements," *IEEE Transactions on Power Delivery,* Vol. 3, No. 4, 1326–1333, October 1988.
5. Iabridis, D., and P. Dokopoulos, "Finite element computation of eddy current losses in a non-linear ferromagnetic sheaths of three-phase power cables," *IEEE Transactions on Power Delivery,* Vol. 7, No. 3, 1060–1067, July 1992.
6. Xu, X.-B., and X. Yang, "A simple computational method for predicting magnetic field in the vicinity of a three-phase underground cable with a fluid-filled steel-pipe enclosure," *IEEE Transactionson Power Delivery,* Vol. 10, No. 1, 78–84, January 1995.
7. Xu, X.-B., and X. Yang, "Computation of magnetic fields generated by an underground pipe-type cable," *IEEE Transactions on Power Delivery,* Vol. 11, No. 2, 650–655, April 1996.
8. Xu, X.-B., and X. Yang, "A hybrid formulation based on unimoment method for investigating the electromagnetic shielding of sources within a steel pipe," *Electromagnetic Waves, PIER I2,* Chapter 6, J. A. Kong (Chief Editor), EMW Publishing, Cambridge, Massachusetts, 1996.
9. Silvester, P. P., and R. L. Ferrari, *Finite Elements for Electrical Engineers* (2nd Edition), Cambridge UniversityPress, 1990.
10. Jin, J., *The Finite Element Method in Electromagnetics,* John Wiley & Sons, Inc., New York, 1993.

11. Xu, X.-B., G. Liu, and P. Chow, "A finite-element method solution of zero-sequence impedance of underground pipe-type cable," *IEEE Transactions on Power Delivery,* submitted for publication.
12. Harrington, R. F., *Time-Harmonic Electromagnetic Fields,* McGraw-Hill Book Company, 1961.
13. Konard, A., "The numerical solution of steady-state skin effect problems-an integrodifferential approach," *IEEE Transaction on Magnetics,* Vol. MAG-17, No. 1, 1148–1152, January.
14. Hatziathanassiou, V., and D. Labridis, "Coupled magneto-thermal field computation in three-phase gas insulated cables," *Archiv fur Electrotechnik,* 76, 285-292, Spring-Verlag, 1993.
15. Labridis, D., and V. Hatziathanassiou, "Finite element computation of field, forces and inductances in underground SF insulated cables using a coupled magneto-thermal formulation," *IEEE Transactions on Magnetics,* Vol. 30, No. 4, 1407–1415, July 1994.
16. Xu, X.-B., and G. Liu, "Application of homogeneous Dirichlet bounding condition in the finite-element analysis o power cables," *IEEE Transactions on Magnetics,* submitted for publication.